Return-Current Heating and Implosion of Cylindrical CO_2-Laser-Driven Targets

A. Hauer and R. J. Mason
Los Alamos National Laboratory, University of California, Los Alamos, New Mexico 87545

(Received 1 April 1983)

The Helios laser system has been used to deliver 2.3 kJ to the capped end of 0.75-mm-long, 130-μm-diam hollow rods of 5-μm wall thickness. Soft-x-ray pinhole pictures demonstrate the cylindrical implosion of these targets. The measured 130-eV core temperatures from the filtered pictures and the 7×10^6-cm/s collapse velocity from optical streak photographs are consistent with heating by a 0.8×10^6-A return current, representing the recycling of 15% of the hot-electron emission.

PACS numbers: 52.50.Jm, 52.25.Fi, 52.30.+r, 52.70.-m

At intensities which exceed 10^{15} W/cm^2 most of the energy absorbed from CO_2 lasers goes directly into a relatively small number of highly energetic (>200 keV) suprathermal electrons.[1] This energy must be transferred to a much larger number of localized thermal electrons to accomplish laser fusion. Since direct classical coupling of the suprathermals to the background plasma has proven inefficient, we have initiated an effort to use the self-generated fields in specialized targets to improve the energy transfer. Charge imbalance develops as suprathermals leave a laser spot. The resultant E fields can draw a return current, if an appropriate path is provided. Benjamin *et al.*[2] have demonstrated the existence of these currents, and their ability to heat a target support stalk. This Letter reports the first experimental results from targets designed to use the return currents to heat and implode a thin-walled hollow cylinder—to produce a micro Z pinch.

A schematic of the "augmented return current" (ARC) targets used in the experiments is given in Fig. 1. Four tightly focused CO_2-laser beams from the Los Alamos Helios laser system impinge on the capped end of a long hollow, low-Z cylinder, coated with a thin layer of metal (gold or aluminum). The cylinder is mounted at the center of a large high-Z disk. Suprathermals generated at the focus will drift toward the disk in the plasma surrounding the cylinder. A thermal return current is drawn back along its walls. Resistivity of the walls results in Joule heating of the thermals. The B field from the resultant current loop can implode and further heat the cylinder.

Experiments were performed on targets with a variety of diameters and lengths. The smallest cylinders were matched to the minimal laser spot diameter. Their length was set at roughly 5 diameters to maximize the aspect ratio for current-related effects, under the constraint of minimum mass—for maximum temperature gain from energy deposition. The minimum wall thickness was set by limits on structural integrity. The metal layer was added to provide a brighter signature in x-ray pinhole pictures. The earlier experiments[2] recorded currents from electrons escaping to the walls of the target chamber. The ARC targets were designed to augment this current through the axial alignment of the cylinder and beams, with a cylinder much thicker than the earlier 10-μm stalks, and with the addition of the collector disk for possible suprathermal entrainment. The presence of thermoelectric, $\nabla n \times \nabla T$ B fields has been recognized for some time.[3-6] The cylindrical return currents and any pinch effect should serve to enhance these fields. Suprathermal drift down the cylinder[7] is consistent with a B field, directed as in Fig. 1, and with an outwardly directed E field for containment of the electron cloud. The axial E-field component, drawing the return current against resistivity, introduces a "tilt" in the $E\times B$ drift, which should aid capture of the suprathermals by the cylinder wall. Alternatively, the B field around the cylinder should help to shield its interior from suprathermal preheat.[8] The return-current effects discussed here will be reduced to the extent that deposited energy is lost to fast-ion blowoff. However, cylindrical geometry may serve to reduce fast-ion losses, as compared to those from foils,[6] since the area

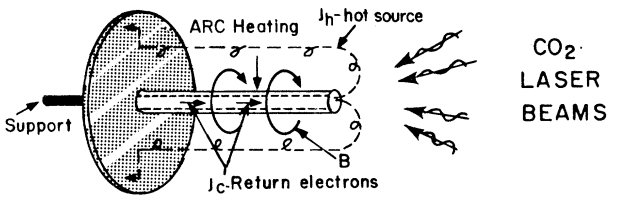

FIG. 1. Sketch of the ARC target design.

© 1983 The American Physical Society

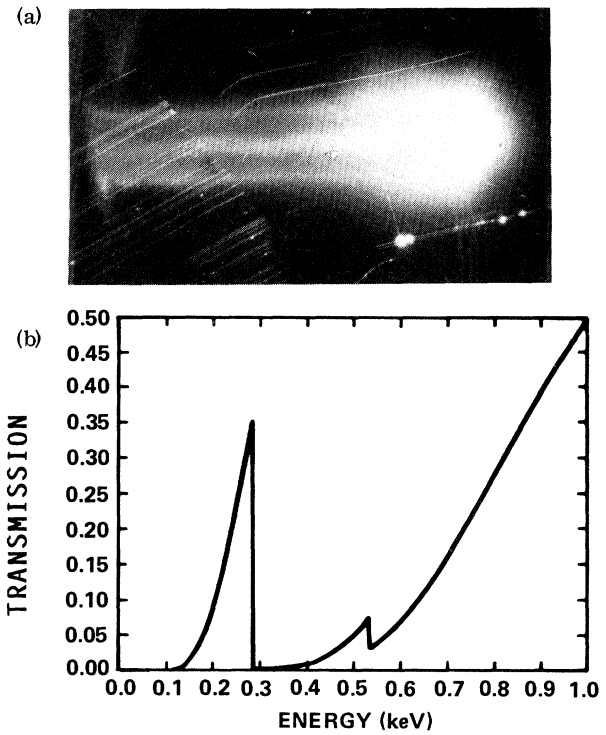

FIG. 2. (a) Soft-x-ray pinhole image showing the initial wall position of a 260-μm-diam ARC target and its imploded core; (b) filter transmission for the pinhole channel producing the image in (a).

for fast-ion emission increases only linearly with distance along the axis.

The experimental ARC cylinders were plastic, 130 to 500 μm in diameter, and 750 to 1500 μm in length. The cap and wall thickness ranged from 3 to 5 μm. The metal layer added an extra 0.3 to 1.0 μm of thickness. The disk was of gold, 25 μm thick and 10^3 μm in diameter. The laser delivered a nominal 2.3 kJ to these targets in 0.6-ns pulses. At tight, overlapped focus (providing a 130-μm-diam spot) the intensity was $I = 3 \times 10^{16}$ W/cm^2, of which a fraction $f = 0.6$ was absorbed.

Hard-x-ray measurements[1] set the suprathermal source temperature at $T_h \sim 450$ keV in these experiments. Using the energy balance relation $fIA = (J_h/e)kT_h$, and $A = 1.3 \times 10^{-4}$ cm^{-2} as the end area of the thinnest cylinders, we obtain $J_h = 5.2 \times 10^6$ A. Assuming, consistent with the experimental results which follow, that 15% of the emitted current is recycled, we determine a return current of 0.8 MA. This yields a surface field $B = 0.2J(\mathrm{A})/r(\mathrm{cm})$ of 24×10^6 G, and a magnetic pressure, $p_B = B^2/8\pi$, of 23 Mbar. For comparison, the emitted-hot-electron pressure is 6.5 Mbar, and the fully ionized perfect-gas plastic pressure at 50 eV (characteristic of the early wall conditions—see below) is $P_c = 15$ Mbar. The mass of the 5-μm plastic and 0.3-μm gold in the cylinders was 1.5 and 1.7 μg, respectively. If this is accelerated under the 23-Mbar magnetic pressure to a 20-μm minimum radius (ignoring pulse shape, B-field compression, and back-pressure effects), the average velocity achieved is 7×10^6 cm/s, and the transit time is 630 ps. Upon central collapse of the cylinder this velocity implies a temperature rise over preheat conditions in the gold (for an effective ionization of $Z = 27$) of 113 eV. Alternative calculations balancing the Joule heating in the gold with blackbody losses from its surface lead to a similar estimated temperature rise.

An important diagnostic in the experiments was the soft-x-ray imaging, performed with an array of filtered pinhole cameras. Figure 2(a) shows a typical image (for shot 3, Table I) from a camera viewing perpendicular to the target axis. The bright oval feature at the right is the region of laser incidence. The two outermost parallel lines to the left are the heated cylindrical walls. Between these lies the imploded core —displaying a twist reminiscent of magnetic kink instability. In Fig. 2(b) is the filter transmission for the x-ray channel yielding the image in Fig. 2(a). By examining several images with different filtration, estimates of the initial wall and the

TABLE I. Imploded core temperature as determined by x-ray imaging.

Shot No.	Laser energy (J)	Target length (μm)	Target diameter (μm)	Coating type/thickness (μm)	Imploded core temperature (eV ± 30)
1	2367	750	130	Au/0.3	135
2	2526	750	130	Au/0.3	140
3	2315	1500	260	Al/2.0	120
4	2384	1500	260	Au/0.3	130

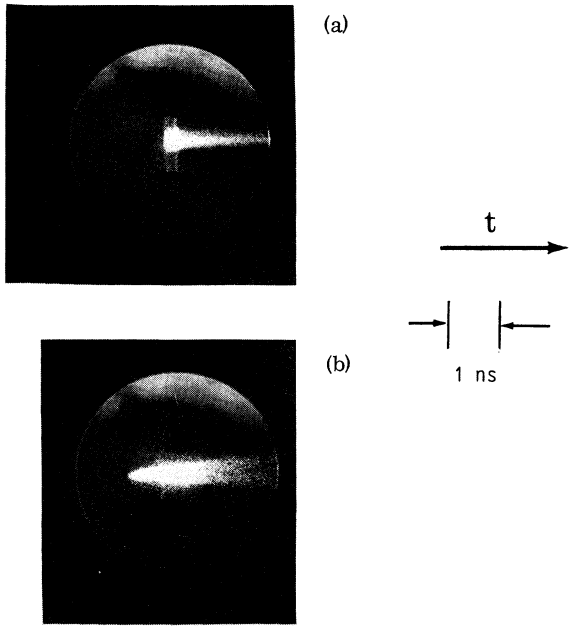

FIG. 3. (a) Optical streak photograph for the 130-μm-diam ARC target; (b) streak photograph for an exploding pusher (directly suprathermal heated) target, evidencing considerable outgoing material.

imploded-core temperatures can be made.[9] Assuming blackbody emission and making predictions for the various experimental channels, we chose the temperature giving the best overall agreement between these predictions and the observed channel signals. Table I collects results from this analysis for the core temperatures in the various target types employed. The temperatures range from 120 to 140 eV—with the smaller targets hotter.

Optical streak photography provided an additional useful diagnostic. The camera viewed the targets in a direction perpendicular to the cylindrical axis in the same plane as the x-ray imaging. The photograph for shot 2, Table I, is shown in Fig. 3(a). The collection system was apertured to cover only the cylinder, excluding the laser absorption region. Camera filtering emphasized radiation toward the blue end of the spectrum. A maximum speed of (5 to 7) $\times 10^6$ cm/s is indicated by the photograph.

Two observations strongly suggest that the heating and implosion of the cylinders is due to return currents rather than direct electron deposition. First, the optical streak photographs show primarily inward flowing material. In contrast, photographs of directly heated targets show considerable radiation from outward flowing material, as demonstrated by Fig. 3(b). The thickness of the ARC cylinder walls is such that direct heating by the $T_h \geq 100$ keV suprathermals would give essentially explosive behavior (with equal material moving in and out). The second observation involves the soft-x-ray images themselves [such as Fig. 2(a)]. Soft-x-ray photos ($h\nu \leq 1$ keV) of exploding pushers show very weak (if any) evidence of the imploded core. This is because very soft radiation from the core is either masked by the strong coronal radiation or is absorbed. A typical soft-x-ray photo of an exploding pusher implosion is shown in Fig. 4. The signature of the exploding pusher core is lacking (despite a strong implosion for the target), whereas the subkilovolt ARC photographs display the core vividly.

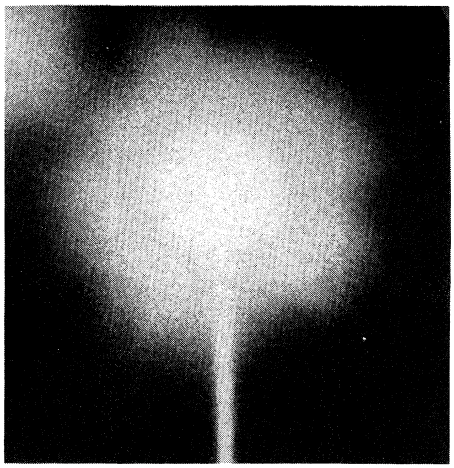

FIG. 4. Soft-x-ray photograph of a typical CO_2-laser-illuminated spherical exploding pusher at $I > 5 \times 10^{15}$ W/cm^2 showing little record of the compressed core.

Although it appears that the desired target behavior has been generally achieved, the actual energy transfer to thermals remains small. Only 21 J is required to raise the entire cylindrical 3.2-μm mass to 130 eV. We anticipate that the coupling can be improved by lowering the temperature of the suprathermals. A threefold reduction of T_h to 150 keV should raise the return current correspondingly—for a ninefold increase in magnetic pressure and a substantial increase in the collapse velocity. A reduced T_h could come from flattening the illuminated cap into a "nail head," displaying an increased area for an appropriately decreased laser intensity with defocused beams.

In conclusion, we have shown that CO_2 lasers

can be used to induce the cylindrical implosion of end-illuminated targets, and that the implosion characteristics are consistent with heating due to a return current. Laser-driven pinches like these could be used to test pulsed-power concepts. The production of a long thin high-density plasma column may also prove useful in experiments designed to observe gain[10] in the x-ray region of the spectrum.

The authors wish to acknowledge encouraging and stimulating discussions with Robert Benjamin and Sidney Singer. The difficult fabrication of these targets was accomplished by the Los Alamos fabrication team. We are also grateful to the Helios laser operations group. This work was performed under the auspices of the U. S. Department of Energy.

[1]W. Priedhorsky, D. Lier, R. Day, and D. Gierke, Phys. Rev. Lett. 47, 1661 (1981). Extensive comparisons between numerical hydrodynamical simulations and experiment indicate that the hot-electron–generation temperature is roughly twice the slope of the hard–x-ray spectrum. This was the value taken for the present work.

[2]R. F. Benjamin, G. H. McCall, and W. Ehler, Phys. Rev. Lett. 42, 890 (1979); see also R. F. Benjamin, J. S. Pearlman, E. Y. Chu, and J. C. Riordan, Appl. Phys. Lett. 39, 848 (1981).

[3]J. A. Stamper and B. H. Ripin, Phys. Rev. Lett. 34, 138 (1975); J. A. Stamper, E. A. McLean, and B. H. Ripin, Phys. Rev. Lett. 40, 1177 (1978).

[4]R. Serov and M. C. Richardson, Appl. Phys. Lett. 28, 115 (1976).

[5]R. J. Mason, Phys. Rev. Lett. 42, 239 (1979).

[6]D. W. Forslund and J. U. Brackbill, Phys. Rev. Lett. 48, 1614 (1982); M. A. Yates, D. B. van Hulsteyn, H. Rutkowski, G. Kyryla, and J. U. Brackbill, Phys. Rev. Lett. 49, 1702 (1982).

[7]P. A. Jaanimagi, N. A. Ebrahim, N. H. Burnett, and C. Joshi, Appl. Phys. Lett. 38, 734 (1981).

[8]R. F. Benjamin, Los Alamos National Laboratory Report No. LA-UR-81-3722 (unpublished).

[9]The technique employed is the imaging analog of the well-known procedure for measuring radiation temperature. See, for example, H. Griem, *Plasma Spectroscopy* (McGraw-Hill, New York, 1964).

[10]R. C. Elton, Optical Eng. 21, 307 (1982).

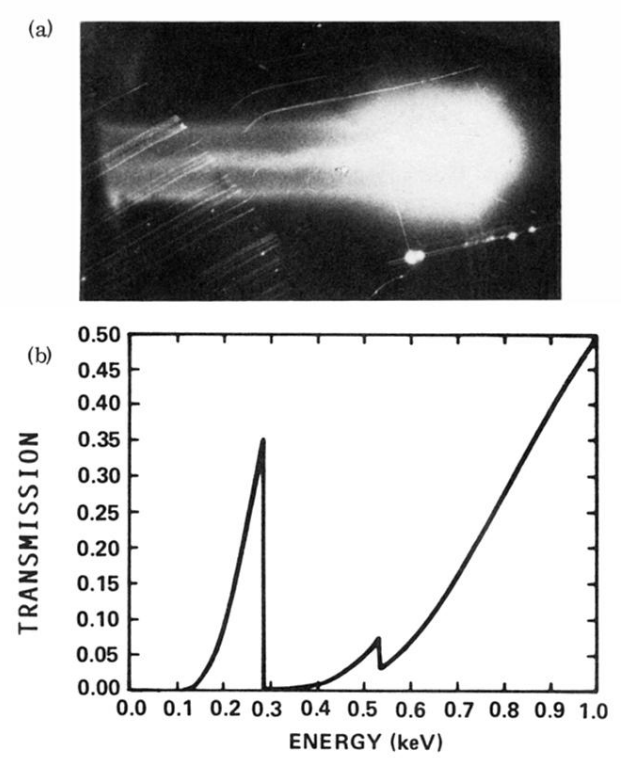

FIG. 2. (a) Soft-x-ray pinhole image showing the initial wall position of a 260-μm-diam ARC target and its imploded core; (b) filter transmission for the pinhole channel producing the image in (a).

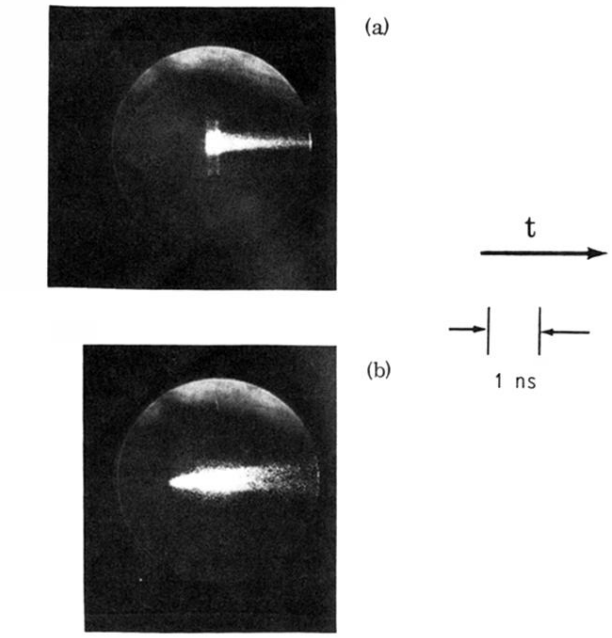

FIG. 3. (a) Optical streak photograph for the 130-μm-diam ARC target; (b) streak photograph for an exploding pusher (directly suprathermal heated) target, evidencing considerable outgoing material.

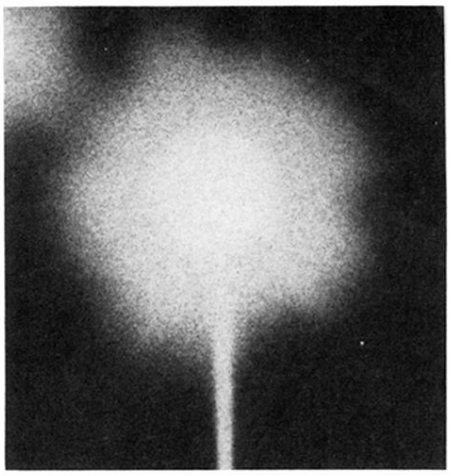

FIG. 4. Soft–x-ray photograph of a typical CO_2-laser–illuminated spherical exploding pusher at $I > 5 \times 10^{15}$ W/cm^2 showing little record of the compressed core.